General Disclaimer

- This document has been reproduced from the best copy furnished by the organizational source. It is being released in the interest of making available as much information as possible.

- This document may contain data, which exceeds the sheet parameters. It was furnished in this condition by the organizational source and is the best copy available.

- This document may contain tone-on-tone or color graphs, charts and/or pictures, which have been reproduced in black and white.

- This document is paginated as submitted by the original source.

- Portions of this document are not fully legible due to the historical nature of some of the material. However, it is the best reproduction available from the original submission.

NASA Technical Memorandum 86915

Fundamental Tribological Properties of Ceramics

Donald H. Buckley and Kazuhisa Miyoshi
Lewis Research Center
Cleveland, Ohio

Prepared for the
Ninth Annual Conference on Composites and Advanced Ceramic Materials
sponsored by the American Ceramic Society
Cocoa Beach, Florida, January 20-24, 1985

NASA

FUNDAMENTAL TRIBOLOGICAL PROPERTIES OF CERAMICS

Donald H. Buckley and Kazuhisa Miyoshi
National Aeronautics and Space Administration
Lewis Research Center
Cleveland, Ohio 44135

SUMMARY

When a ceramic is brought into contact with itself or another ceramic, or a metal, strong bond forces can develop between the materials. The bonding forces will depend upon the state of the surfaces, cleanliness, and the fundamental properties of the two solids, both surface and bulk. Adhesion between a ceramic and itself or another solid are discussed from a theoretical consideration of the nature of the surfaces and experimentally by relating bond forces to the interface resulting from solid-state contact. Elastic, plastic, and fracture behavior of ceramics in solid-state contact are discussed as they relate to friction and wear. The contact load necessary to initiate fracture in ceramics is shown to be appreciably reduced with tangential motion. Both friction and wear of ceramics are anisotropic and relate to crystal structure as with metals. Grit size effects in two and three body abrasive wear are observed for ceramics. Both free energy of oxide formation and the d valence bond character of metals are related to the friction and wear characteristics for metals in contact with ceramics. Surface contaminants effect friction and adhesive wear. For example, carbon on silicon carbide and hydrogen on aluminum oxide reduce friction while oxygen on metal surfaces in contact with ceramics increase friction. Lubrication is found to increase the critical load necessary to initiate fracture of ceramics with sliding or rubbing contact.

INTRODUCTION

Ceramics like metals when in the atomically clean state will exhibit strong bonds of adhesion. This will occur for ceramics in contact with themselves and other materials. There are a number of both bulk and surface properties of ceramics that will affect the nature and magnitude of the adhesive bond forces that develop for ceramics. With respect to surface properties these include electronic surface states, ionic species present at the surface, chemistry of the contacting material and the nature of surface contaminants present. Bulk properties include crystallography, cohesive binding energy and the presence or absence of defects.

Considerable effort has been put in fundamental studies of adhesion, friction, and wear of metals. In recent years the increasing potential for the use of ceramics as components in lubrication systems has focused attention on these materials. Adhesion, friction, and wear studies have been conducted with ceramic materials to better understand their physical and chemical properties which will effect their behavior when in contact with themselves, other ceramics, or metals.

Metals generally readily deform plastically, whereas ceramics, while having high strength, are normally brittle and fracture with little or no

evidence of plastic flow. At the interface between two ceramics in solid state contact under load and relative motion, plastic flow has been observed in the surface layers of some ceramics.

The factors which influence the mechanical behavior of materials when plastic flow occurs such as crystal structure, dislocations, vacancies, and stacking faults, can therefore be expected to influence the adhesion, friction, and wear behavior of ceramics and comparisons can be made between ceramics and metals.

The presence of surface films such as adsorbates markedly influence the adhesion, friction, and wear behavior of metals and ceramics as well. Further, with ceramics and other ionic solids, the presence of surface films such as water and surface active organics can influence adhesion, friction, and wear by altering the amount of plastic deformation that will occur during sliding or rubbing.

The objectives of this paper are to review the adhesion, friction, and wear of ceramics, anisotropic friction and wear behavior, and the effect of surface films and ceramic-metal interactions. Analogies to metals will be made where applicable. Both oxide and nonoxide ceramics will be discussed.

RESULTS AND DISCUSSIONS

Oxide Ceramics

Oxides such as aluminum oxide, titanium oxide (rutile), and magnesium oxide have been considered for tribological applications. With these materials, both structure and surface chemistry are extremely important to adhesion behavior.

Aluminum oxide. - In order to determine if friction and accordingly adhesion characteristics of sapphire (aluminum oxide) were anisotropic, experiments in vacuum were conducted with two orientations of a sapphire ball. The first orientation involved the plane (0001) and the directions $[11\bar{2}0]$ and $[10\bar{1}0]$ and the second the $(10\bar{1}0)$ plane with sliding in the $[11\bar{2}0]$ and [0001] directions in adhesive contact and sliding against a disk of sapphire with its basal plane essentially parallel (within 4°) to the interface. The results obtained in these experiments are presented in table I.

The influence of crystallographic direction for both prismatic and basal orientations are seen in table I. With the basal orientation less adhesion and a lower coefficient of friction was observed in the preferred slip direction $[11\bar{2}0]$. This orientation dependence is similar to that observed for the hexagonal metal berryllium in reference 1.

The results of table I indicate that the adhesion and friction characteristics of sapphire are highly anisotropic. There was further, marked evidence for plastic deformation at the contacting interface of the crystals as revealed by etching of sapphire crystals after the friction experiments. The adhesion and friction behavior of sapphire in the table is very analogous to that observed with hexagonal metals in Refs. 2 and 3. With hexagonal metals in sliding friction experiments the friction coefficient was always less on

preferred slip planes in preferred slip directions than for other slip systems. Similar results were obtained in this investigation. The easy glide or slip plane for sapphire is the basal plane under deformation. Further the preferred slip direction is the $[11\bar{2}0]$ direction when the crystal is deformed plastically. With plastic deformation occurring at the contacting interface under an applied load it might be anticipated that the prismatic orientation of sapphire would exhibit stronger adhesion and higher coefficients of friction than the basal orientation. There are a number of prismatic planes which can slip in the deformation process while, with the basal plane oriented parallel to the sliding interface, only a single set of planes are involved.

When plastic deformation occurs at the sliding interface and a larger number of slip planes are involved, applied stresses in the form of the load may be distributed over a number of equivalent planes. With the basal plane parallel to the sliding interface, any applied normal load can only tend to compress basal planes and even with metals such as beryllium, this orientation will support tremendous loads to the point where it will literally explode with no evidence of slip occurring on other slip planes. A larger true contact area can then occur in the sliding process with prismatic than with the basal orientation. Further, when a number of prismatic planes undergo slip, there exists the possible interaction of such slip planes to produce locks similar to the Lomer-Cottrell locks observed in the face centered cubic metals. Such locks can produce marked increases in shear strength.

With sapphire the yield point for the prismatic orientation is different than that for the basal orientation. For the latter orientation the yield stress is ten times less at elevated temperatures (ref. 4).

The shear strength for sapphire calculated from adhesion and friction measurements of this investigation together with bulk shear strength data obtained from reference 4 are presented in table II. The surface shear strength is from 20 and 30 times that of the bulk shear strength. Similar results have been observed with a number of inorganic crystals in reference 5. A possible explanation for this increase may be that indicated in reference 4. Microscopic plastic deformation occurring at the sliding interface permits relief of stresses in the sapphire resulting in an increase in shear strength.

When hard oxide ceramics are in solid-state contact with softer materials such as metals the marked difference in elastic and plastic deformation of the two materials can result in plowing of the softer material. This, then can contribute to the wear of one or both materials. In figure 1 a rider (hemisphere) of sapphire slid on a single crystal flat of copper. The specimen materials were then reversed so that a single crystal copper rider slid on a sapphire flat. The coefficient of friction for the sapphire sliding on copper was 1.5. With copper sliding on sapphire, it was 0.2. In both instances, adhesion of copper to sapphire occurred. The difference in friction coefficient for the two experiments is due to the effects of plowing (ref. 6).

In both experiments the sapphire underwent wear as indicated in the photomicrographs of figure 1. The wear on the sapphire flat was occasioned by fracture along {0001} planes and subsurface and parallel to the sliding interface. When metals contact hard oxide ceramics, surface chemistry plays a very important role in the observed friction and wear behavior. Various

metals were slid on a flat of sapphire with the basal orientation in the sapphire parallel to the sliding interface. With the metals which form stable oxides such as copper, nickel, rhenium, cobalt, and beryllium, adhesion of the metal occurred to the oxygen ions in the outermost atomic layer of the sapphire. The manner of bonding is shown in figure 2.

When the same sliding experiments are conducted with metals that do not form stable oxides in vacuum (gold and silver) strong chemical bonding does not occur at the interface, adhesion is weak, and wear to the hard oxide ceramic is absent. This is demonstrated in the data of figure 3 for gold and silver sliding on the basal orientation of sapphire.

The photomicrographs of figure 3 indicate an absence of any wear to the sapphire such as observed in figure 1 with copper. The only surface markings in figure 3 were polishing scratches. The coefficients of friction for gold and silver sliding on sapphire were also one-half in figure 3 of that observed with copper sliding on sapphire in figure 1. In figure 1 fracture occurs in the sapphire because in the interfacial metal to the sapphire bond strength is greater than the cleavage or fracture strength in the sapphire and accordingly sapphire wear occurs. With gold and silver in figure 3, the weakest region is the interface and simple shear takes place here with bond strength no stronger than found with lubricant molecules as evidenced by the friction coefficient of 0.1 which is comparable to that experienced with effective boundary lubrication.

Experiments subsequent to those of reference 6 confirmed a chemical bond between metals and the oxygen ions indicated in figure 2 (ref. 7). The shear strength of the metal to sapphire contact were correlated with the free energy of formation of the metal oxide in reference 7.

Further attempts have been made to explain in a more fundamental manner the metal to sapphire bonding. This could assist in understanding the wear of hard ceramic oxides in general. Molecular-orbital energies have been examined for clusters in bulk sapphire and the metal-sapphire interface (ref. 8). Figures 4 and 5 represent an attempt to explain the bonding mechanism in greater detail (ref. 8).

The primary interaction at the metal-sapphire interface, as revealed by the studies occurs between the metal d orbitals and otherwise nonbonding p orbitals of the oxygen ions at the surface of the sapphire crystal, i.e., the nonbonding p orbitals at the top of the valence band. It will be noticed in figure 4 that the d-orbital energies of the isolated metal atoms, as determined by this method, are in close proximity to the sapphire valence band, and the position of the atomic level relative to the top of the valence band changes systematically through the series Fe, Ni, Cu, and Ag. The metal-sapphire contact interaction produces at the interface manifolds of spatially localized occupied metal (d)-oxygen(p) bonding molecular orbitals of energies near the bottom of the sapphire valence band and metal(d)-oxygen(p) antibonding molecular orbitals of energies near the top of the sapphire valence band, as exemplified for Fe by the bonding and antibonding orbital wave-function contour maps in figure 5(a) and (b), respectively. For Fe and Ni, the antibonding orbitals are only partially occupied and are located well above the valence band within the band gap, as shown in figure 4. For example, the antibonding Fe(d)-O(p) orbital mapped in figure 5(b) is unoccupied. For Cu and Ag, the antibonding orbitals are fully occupied and are located close to the top of

the valence band. In addition to this covalent bonding and antibonding interactions between the metal and sapphire substrate, there is an ionic component associated with metal-to-oxygen charge transfer at the metal-sapphire interface. These results on covalent and ionic interactions indicate that a chemical bond is in fact established between metal atoms and the oxygen anions on the sapphire surface, and that the ionic component of bonding is proportional to the metal(d) and oxygen(p) orbital electronegativity difference.

Relative to the strength of this bond, it is well known from the most elementary principles of quantum chemistry that the occupation of antibonding molecular orbitals tends to cancel the effects of occupied bonding orbitals, and reduces the net chemical bond strength in comparison to the situation where only bonding orbitals are occupied. Therefore, the increase in occupancy of the metal-sapphire antibonding orbitals through the series Fe, Ni, Cu, and Ag should tend to lower the net metal-sapphire chemical bond strength, which correlates with the significant reduction in metal-sapphire contact strength measured in adhesion, friction and wear experiments. The decrease of the friction coefficient from 0.2 for Cu to 0.1 for Au or Ag is explained qualitatively by the combined effects of increasing antibonding orbital occupancy and decreasing metal-to-oxygen charge transfer. The relatively small friction coefficients and shear strengths of Au (0.1) and Ag (0.1) are consistent with the fact that the fully occupied antibonding orbitals shown in figure 4 essentially cancel the covalent contributions of the bonding orbitals, leaving only small residual ionic and van der Waals contributions.

Similar studies should be conducted on other oxide ceramics to determine if a general relationship between interfacial bonding and fracture can be developed. This could lead to a better understanding of friction and wear.

Ferrites. - With oxide ceramic materials such as Mn-Zn and Ni-Zn ferrites adsorbates are present on the surface from the environment, and these include water vapor and carbon. With metals, in addition to the presence of adsorbate films, beneath this layer of adsorbate is generally a layer of metal oxide.

The adsorbates play a very large role in adhesion, mechanical and chemical behavior of the ferrite ceramic surfaces in tribological systems. Experiments carried out in two environments, vacuum and argon at atmospheric pressure indicate the effects of adsorbate and environment on adhesion and friction properties. The removal of adsorbed films from the surfaces results in very strong interfacial adhesion and high friction.

The data obtained from the experiments in vacuum are to be anticipated from chemical interactions and the important role they play in the adhesion and friction of clean ferrite-to-metal couples. The behavior is analogous to that observed for aluminum oxide.

The coefficients of friction reflecting interfacial adhesion for various metals sliding on ferrites in argon atmosphere were all nearly 0.1 to 0.2. The chemical activity or inactivity of metal does not appear to play a role as to adhesion and friction in argon as the argon is only physically adsorbed. A prerequisite for this sameness in friction is that the metals form a stable metal oxide, and the environment is responsible for providing the adsorbates on the surface.

Similiar experiments with ferrites contacting polymeric magnetic type indicate that adsorbed nitrogen will appreciably reduce adhesion and accordingly friction. Oxygen conversely increases adhesion and friction.

The adhesion and accordingly coefficients of friction for polycrystalline Ni-Zn and Mn-Zn ferrites in contact with metals can be correlated with the free energy of formation of the lowest metal oxides, as shown in figure 6. The correlation shown in figure 6 clearly indicates that the metal-ferrite adhesive bond at the interface is primarily a chemical bond between the metal atoms and the large oxygen anions in the ferrite surface, and the strength of this bond is related to oxygen to metal bond strength in the metal oxide (ref. 9).

All metals indicated in figure 6 adhered and transferred to the surface of the ferrites. In general the less active the metal, the less adhesion and transfer there is to the ferrite. Titanium, having a much stronger chemical affinity to the elements of the ferrite, exhibited the greatest amount of transfer (ref. 10).

The relative chemical activity of the transition metals (metals with partially filled d shells) as a group can be ascertained from their percentage d-bond character, as established by Pauling (ref. 11). The frictional properties of metal-metal and metal-nonmetal contacts have been shown to be related to this character (refs. 12 to 15). The greater the percentage of d-bond character, the less active is the metal, and the lower is the adhesion and friction. Conversely, the more active the metal, the greater is the adhesion.

The coefficients of friction for various metals in contact with Ni-Zn ferrites are replotted with solid symbols in figure 7 as a function of the d-bond character of the transition metal. Titanium, which is a chemically active metal, exhibits a considerably higher coefficient of friction in contact with ferrite than does rhodium, which is a metal of lesser activity.

Figure 7 also presents the coefficient of friction for various metals in contact with the ferrites, in which both metal and ferrite specimens were exposed to O_2 gas (99.99 percent pure). The data reveal increase in adhesion and the coefficients of friction for Ni-Zn ferrite-to-metal interface.

NONOXIDE CERAMICS

The high strength and excellent oxidation and creep resistance of nonoxide ceramics such as silicon carbide make them extremely important materials for high-temperature mechanical and electronic applications in severe environments. Materials such as silicon carbide are used for example, in stable high-temperature semiconductors, in gas turbine blades, in turbine ceramic seals, and as an abrasive for grinding (refs. 16 and 17).

Much like oxide ceramics the nonoxide ceramics exhibit anisotropic behavior in many of their mechanical properties. Friction and wear behavior of nonoxide ceramics are also anisotropic under both adhesive and abrasive conditions.

Silicon Carbide. - Anisotropy results can be of two kinds. First, there is the observed variation of friction and wear when the sliding surface is

changed from one crystal plane to another for a given material. Secondly, there is the variation of friction and wear observed when the orientation of sliding surface is changed with respect to a specific crystallographic direction on a given crystal plane as reported for aluminum oxide in table I. For example, the differences in coefficients of friction with respect to the mating crystallographic planes and directions are significant under adhesive conditions as was indicated for sapphire in table I. The data of table I were obtained in vacuum with clean aluminum oxide. The lowest coefficients of friction were obtained for aluminum oxide in table I on the preferred slip plane when sliding in the preferred slip direction. Similar results have been obtained with silicon carbide. Their anisotropic friction is shown in table III. Again, the lowest coefficients of friction with silicon carbide were obtained on the preferred basal slip plane when sliding in the preferred $\langle 11\bar{2}0 \rangle$ slip direction. The coefficient of friction reflects the force required to shear at the interface with the basal planes of the silicon carbide parallel to the interface. The results presented in table III indicate that the force to resist the shearing fracture of the adhesion bond at the interface is lower in the preferred crystallographic $\langle 11\bar{2}0 \rangle$ direction than it is in the $\langle 10\bar{1}0 \rangle$ direction.

Under abrasion just as under adhesive conditions the differences in the coefficients of friction and wear with respect to the crystallographic plane and direction were also significant. In this case, plowing was extremely important and influenced the friction and wear when ceramics contacted hard materials. With silicon carbide the $\langle 10\bar{1}0 \rangle$ directions on the basal {0001} plane exhibited the lowest coefficient of friction and the greatest resistance to abrasion resulting from plastic deformation, as indicated in table IV. The anisotropic friction and wear on the {0001}, $\{10\bar{1}0\}$, and $\{11\bar{2}0\}$ planes of silicon carbide were primarily controlled by the slip system $\{10\bar{1}0\}\ \langle 11\bar{2}0 \rangle$ and were explained by a resolved shear stress calculation (ref. 18).

With ceramic materials adsorbates are present on the surface from the environment, as already mentioned. The adsorbates play a very large role in mechanical and chemical behavior of silicon carbide surfaces in tribological systems.

Typical friction results of silicon carbide surfaces in contact with iron as a function of sliding temperatures are indicated in figure 8. The iron was argon-ion-sputter cleaned before the friction experiments in order to remove adsorbed films and oxides on the iron. The silicon carbide flat specimen was as-received.

Figure 8 indicates the coefficients of friction of the silicon carbide surface in contact with iron as a function of sliding temperatures. The iron rider was sputter-cleaned with argon ions. At temperatures below 400 °C, after the specimen was heated to the sliding temperature, the coefficient of friction increased slightly with further increases in temperature. The coefficient of friction remained relatively unchanged with increasing temperature in range 400 to 800 °C. The general increase in friction at these temperatures (400 to 800 °C) was due to the removal of the contaminants carbon and oxygen from the surface. The increase in friction at these temperatures was associated with increased adhesion and plastic flow in the area of contact. Above 800 °C the coefficient of friction decreased rapidly with an

increase of temperature. The rapid decrease in friction above 800 °C correlated with the graphitization of the silicon carbide surface.

Figure 9 presents the surface chemistry of silicon carbide analyzed by XPS. The as-received crystal was heated at various temperatures in a vacuum.

The Si_{2p} photoelectron peak energies are associated with silicon carbide at various temperatures. The photoelectron lines for C_{1s} of the silicon carbide surface are split asymmetrically into double energy peaks. The results show a significant influence of temperature on the SiC surface. The double energy peaks are due to distinguishable kinds of carbon: (1) a carbon contamination peak and a carbide peak at room temperature, and (2) the graphite and the carbide peaks at temperature form 400 to 1500 °C.

At room temperature and 250 °C, the primary peaks were the adsorbed amorphous carbon contamination and carbide. For specimen heated to 400 °C the carbon contamination peak disappears from the spectrum. Above 400 °C both the peak heights of graphite and the carbide are increased with an increase of heating temperature. A large carbide peak was distinguished at 800 °C. At 900 °C the carbide peak height was smaller than that at 800 °C, but the graphite peak height was larger. At 1000 °C the height of the carbide peak decreased and became smaller than that of the graphite. At 1500 °C the height of carbide peak became very small, but a very large graphite peak was observed. The results indicate that temperature affects significantly the surface chemistry and the surface of silicon carbide graphitizes.

A depth profile into the surface layers for elements present in silicon carbide surface preheated at 1500 °C was obtained as a function of sputtering time and is presented in figure 10. The graphite peak decreases rapidly in the first 30 min of sputtering, and thereafter it gradually decreases with an increase in the sputtering time to about 18 hr. After 18 hr the graphite peak does not change much with sputtering time. On the other hand, the silicon and carbide-carbon peaks increase gradually with increasing sputtering time to 20 hr.

Ellipsometeric measurements have been conducted with two different (0001) faces of the silicon carbide crystals, one which consisted of silicon atoms (0001) and the other which consisted of carbon atoms (0001) at temperatures above 1200 °C. In 1 hr of heating at 1300 °C the layer, which consists of carbon (graphite), on the C-face grows to about 100 nm, whereas the layer on the Si-face did not grow thicker than 10 nm even with longer heating.

The silicon carbide {0001} surfaces used in this investigation consisted of both silicon atoms and carbon atoms because etching silicon carbide surface in molten salt $1NaF + 2KCO_3$ gives both a smooth surface for the Si-face and a rough one for the C-face. The apparent thickness of the layer, which consists of graphite at the surface and is produced by heating above 1200 °C for 1 hr, is about 100 nm (1000 Å), and it is equivalent to a depth of a layer sputter etched for about 18 hr shown in figure 10.

The low friction and wear at the high temperatures appears to correlate with the graphitization of the silicon carbide surface. The coefficients of friction on this surface at the high temperatures are nearly the same as those

on pyrolytic graphite in sliding contact with single-crystal iron in the vacuum of 10 nPa.

The removal of adsorbed films (usually water vapor, carbon monoxide, carbon dioxide, and oxide layers) from the surfaces of ceramics and metals results in very strong interfacial adhesion when two such solids are brought into contact. For example, when an atomically clean silicon carbide surface is brought into contact with a clean metal surface, the adhesive bonds formed at the silicon carbide-to-metal interface are sufficiently strong that fracture of cohesive bonds in the metal and transfer of metal to the silicon carbide surface results. This is observed in the scanning electron microscope.

Figure 11 presents scanning electron photomicrographs of the wear tracks generated by 10 passes of rhodium and titanium riders on the SiC (0001) surface along the $[10\bar{1}0]$ direction. Metal transfer is evident in the sliding contact. The sliding of a metal on a silicon carbide surface also results in local cracks along cleavage planes. The cracks, which are observed in the wear tracks, primarily propagate along cleavage planes of the $\{10\bar{1}0\}$ orientation. In figure 11(a), the hexagonal light area is the beginning of a wear track, and there is a large crack where cracks primarily along the $\{10\bar{1}0\}$ planes were generated, propagated, and then intersected during loading and sliding of the rhodium rider on the SiC surface. It is postulated from figure 11(a) that subsurface cleavage cracking of the (0001) planes, which are parallel to the sliding surface, also occurs. Figure 11(b) reveals a hexagonal pit and a copious amount of thin titanium film around the pit.

The relative chemical activity of the transition metals (metals with partially filled d shells) as a group can be ascertained from their percentage d-bond character, as established by Pauling (ref. 11). The frictional properties of metal-ceramic (such as BN, SiC, and ferrites) contacts have been shown to be related to this character by the present authors. The greater the percentage of d-bond character, the less active is the metal, and the lower is the friction. Conversely, the more active the metal, the higher is the coefficient of friction. This is demonstrated in figure 12. The coefficients of friction for some transition metals (Ti, Zr, V, Co, Pt, Ni, Fe, Cr, Re, Rh, and W) in contact with the silicon carbide surface decreases with an increase in d-bond character. Titanium and zirconium, which are chemically very active, exhibited very strong interfacial adhesive bonding to the silicon carbide. In contrast, rhodium and rhenium, which have a very high percentage of d-bond character, have relatively low coefficients of friction.

All the transition metals examined failed either in tension or in shear and transferred to the surfaces of silicon carbide, because the interfacial bonds are generally stronger than the cohesive bonds in the metals. In other words the weakest bond in the interfacial region was the metal bond. Therefore, friction properties should correlate with the tensile and shear properties of these metals as well.

There appeared to be a general correlation between the coefficient of friction and the theoretical shear strength of metals, as indicated typically with solid symbols in figure 12. The higher the shear strength, the lower the friction. The morphology of metal transfer to the ceramic material revealed that much more transfer occurred with the metals that have low strength and a low percent d-bond character than with those having higher values.

ADSORBED FILMS

Ceramics like metals are influenced in their tribological behavior by the presence of environmental adsorbates on their solid surfaces. One of the adsorbates present in ordinary air which has a pronounced effect is water. The effect of water vapor on the friction behavior of aluminum oxide is demonstrated, by way of example, in the data of figure 13.

The coefficient of friction is plotted as a function of load in figure 13 for the basal plane of sapphire sliding on itself in air and vacuum. When the specimens are initially placed in vacuum the coefficient of friction is nearly the same as that seen in figure 13 for experiments in air at various loads. The sapphire specimens were then outgassed by electron gas heating. After outgassing the friction coefficients rose to the high values seen in figure 13.

Monitoring of the gases emitted from the aluminum oxide surface while heating revealed the emission of water from the surface. From mass spectrometer data obtained it was therefore concluded that the friction differences seen in figure 13 was due essentially to the presence of absorbed water vapor on the sapphire surface.

LUBRICATION

Lubrication is extremely important to ceramic materials in tribological systems. Not only are adhesion and friction of ceramic materials reduced by the presence of lubricants, but also brittle fracture during sliding, which is one of the main limitations to a wider use of ceramic materials in tribological applications.

Figure 14 presents scanning electron photomicrographs of wear tracks for Mn-Zn ferrite oxide ceramic in sliding contact with a hemispherical (100 μm-radius) diamond rider in dry and under lubricated conditions. The lubricant was an olive oil, which is commonly used in fine lapping processes of ceramic materials and semiconductors. As shown in the photomicrographs, the fracture behavior of the oxide ceramic is very dependent on the lubricant. Cracks generate much more easily in the dry condition than with lubrication.

The tangential force introduced by sliding plays an important role in the generation of surface fracture. The critical load to fracture in dry sliding was one-half of that observed with static indentation. However, under lubricated conditions the critical load to fracture was two times greater than that in dry sliding.

CONCLUDING REMARKS

Based upon fundamental studies conducted with both oxide and nonoxide ceramics the following remarks can be made. Ceramics like metals will deform elastically in the interfacial region between two solids in contact under load. Unlike metals, however, when the elastic limit is exceeded gross fracture, as well as, plastic deformation can occur. With tangential motion the forces necessary to initiate brittle fracture in the ceramic is markedly less than that associated with normal loading.

The friction and wear characteristics of ceramics, again like metals, are anisotropic as reported herein for aluminum oxide and silicon carbide. In general the lowest coefficient of friction is observed when sliding on the preferred slip plane in the preferred slip direction on that plane. Adhesive wear behaves with respect to orientation as does friction. Likewise the high atomic density, most resistant to deformation atomic planes exhibited the greatest resistance to abrasive wear.

Heating of a ceramic such as silicon carbide to high temperatures can result in the graphitization of the ceramic surface with the graphite functioning to reduce abrasion and friction. A lubricating film is therefore provided from the material itself.

Studies with hard oxide ceramics such as aluminum oxide indicate the importance surface atomic bonding mechanisms have both to the wear of the ceramic and ceramic in contact with a metal. With metals contacting the oxide a consideration of molecular-orbital energies and the resulting chemical bonds provide insight into adhesion and adhesive transfer.

With the ferrites contacting metals friction can be related to the free energy of formation of the metals lowest oxide. Friction can also be related to the metal bond character.

Lubrication of ceramic materials generally reduces wear. In a strict sense even adsorbed hydrogen monolayers are lubricants for such surfaces as aluminum oxide and its pressure influences friction. Lubrication of ceramic surfaces increases the critical load to initiate fracture of ceramics, under sliding or rubbing.

REFERENCES

1. Buckley, D.H., Surface Effects in Adhesion, Friction, Wear and Lubrication Elsevier, Amsterdam, 1981.

2. Buckley, D.H., "Effect of Orientation on Friction Characteristics of Single-Crystal Beryllium in Vacuum (10^{-10} Torr)," NASA TN-D-3485, 1966.

3. Buckley, D.H., "Influence of Crystal Orientation on Friction Characteristics of Titanium Single Crystals in Vacuum," NASA TN-D-2988, 1965.

4. Wachtman, J.B. Jr., and Maxwell, L.H., "Strength of Synthetic Single Crystal Sapphire and Ruby as a Function of Temperature and Orientation," American Ceramic Society Journal, 42 No. 9, Sept. 1959, pp. 432-433; see also W.D. Kingery, H.K. Bowen, and D.R. Uhlmann, Introduction to Ceramics, 2nd ed., Wiley, New York, 1976.

5. King, R.F., and Tabor D., "The Strength Properties and Frictinal Behaviour of Brittle Solids," Proceedings Royal Society of London, Series A, Vol. 223, No. 1153, Apr. 22, 1954, pp. 225-238.

6. Buckley, D.H., "Friction Characteristics in Vacuum of Single and Polycrystalline Aluminum Oxide in Contact With Themselves and With Various Metals," ASLE Transactions, Vol. 10, No. 2, Apr. 1967, pp. 134-145.

7. Pepper, S.V., "Shear Strength of Metal-Sapphire Contacts," Journal of Applied Physics, Vol. 47, No. 3, Mar. 1976, pp. 801-808.

8. Johnson, K.H., and Pepper, S.V., "Molecular-Orbital Model for Metal-Sapphire Interfacial Strength," Journal of Applied Physics, Vol. 53, No. 10, Oct. 1982, pp. 6634-6637.

9. Miyoshi, K., and Buckley, D.H., "Properties of Ferrites Important to Their Friction and Wear Behavior," NASA TM-83718, 1984.

10. Miyoshi, K. and Buckley, D.H., "Friction and Wear of Single-Crystal Manganese-Zinc Ferrite," Wear, Vol. 66, No. 2, Feb. 1981, pp. 157-173.

11. Pauling, L., "A Resonating-Valence-Bond Theory of Metals and Intermetallic Compounds," Proceedings, Royal Society of London, Series A, Vol. 196, No. 1046, Apr. 7, 1949, pp. 343-362.

12. Buckley, D.H., "Metal-to-Metal Interface and its Effect on Adhesion and Friction," Journal of Colloid and Interface Science, Vol. 58, No. 1, 1977, pp. 36-53.

13. Miyoshi, K., and Buckley, D.H., "Adhesion and Friction of Single-Crystal Diamond in Contact With Transition Metals," Applications of Surface Science, Vol. 6, No. 2, Oct. 1980, pp. 161-172.

14. Miyoshi, K., and Buckley, D.H., "Friction and Wear Behavior of Single-Crystal Silicon Carbide in Sliding Contact with Various Metals," ASLE Transactions, Vol. 22, No. 3, July 1979, pp. 245-256.

15. Buckley, D.H., "Friction and Transfer Behavior of Pyrolytic Boron Nitride in Contact with Various Metals," ASLE Transactions, Vol. 21, No. 2, Apr. 1978, pp. 118-124.

16. O'Connor, J.R. and Smiltens, J., eds., Silicon Carbide, a High Temperature Semiconductor, Pergamon, New York, 1960.

17. Marshall, R.C., Faust, J.W., Jr., and Ryan, C.E., Silicon Carbide - 1973, Univ. of South Carolina Press, Columbia, 1974.

18. Miyoshi, K., and Buckley, D.H., "Anisotropic Tribological Properties of SiC," Wear, Vol. 75, No. 2, Jan. 15, 1982, pp. 253-268.

19. Meyer, F., and Loyen, G.J., "Ellipsonetry Applied to Surface Problems - Optical Layer Thickness Measurement," Acta Electron, Vol. 18, Jan. 1975, pp. 33-38.

20. Van Bommel, A.J., Crombeen, J.E. and Van Tooren, A., "Leed (low-energy electron diffraction) and Auger Electron Observations of the SiC (0001) Surface," Surface Science, Vol. 48, No. 2, pp. 463-472.

TABLE I. - THE INFLUENCE OF CRYSTALLOGRAPHIC DIRECTION ON THE COEFFICIENT OF FRICTION FOR SAPPHIRE SLIDING ON SAPPHIRE IN VACUUM (30 nPa)

[Load, 10 N; sliding velocity, 0.013 cm/sec.]

Plane	Direction	Coefficient of friction
Prismatic $(10\bar{1}0)$	$[11\bar{2}0]$	0.93
	[0001]	1.00
Basal (0001)	$[11\bar{2}0]$	.50
	$[1\bar{0}\bar{1}0]$	.96

TABLE II. - BULK AND SURFACE SHEAR STRENGTH DATA FOR SAPPHIRE[a]

Source	Shear strength 1×10^6 N/m^2
Bulk shear strength	34.0
Surface shear strength from friction	
(0001) $[11\bar{2}0]$	680.0
$(10\bar{1}0)$ [0001]	1020.0

[a]Surface shear strengths calculated from friction values.

TABLE III. - ANISOTROPIC FRICTION FOR SILICON CARBIDE-SILICON CARBIDE CONTACTS UNDER ADHESIVE CONDITION

Plane	Direction	Coefficient of friction
Basal {0001}	<11$\bar{2}$0>	0.54
	<10$\bar{1}$0>	.68

Load, 0.3 N; sliding velocity, 3 mm/min; vacuum pressure, 10^{-8} Pa; room temperature.

TABLE IV. - ANISOTROPIC FRICTION AND WEAR FOR SILICON CARBIDE UNDER ABRASIVE CONDITION

Plane	Direction	Coefficient of friction	Width of permanent groove corresponding to plastic deformation, μm
{0001}	<1010>	0.19	2.6
	<1120>	.21	2.7
{1010}	<0001>	.29	3.6
	<1120>	.23	2.9
{1120}	<0001>	.31	3.5
	<1010>	.24	3.1

Conical diamond with an apical angle of 117°; Load 0.2 N; sliding velocity, 3 mm/min; in mineral oil; room temperature.

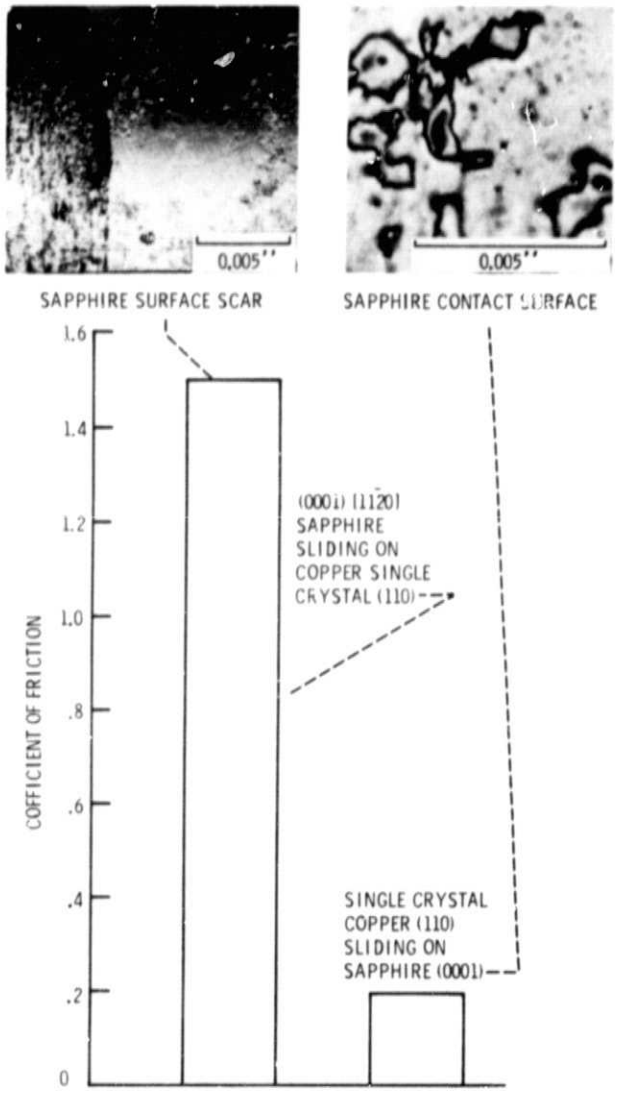

Figure 1. - Coefficient of friction for copper in sliding contact with sapphire in vacuum (10^{-10} torr). Load, 100 g; sliding velocity, 0.013 cm/s.

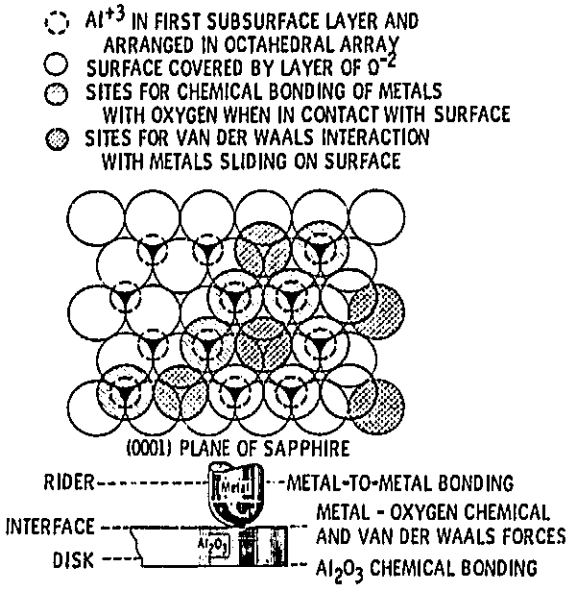

Figure 2. - Nature of surface interaction and bonding of metal to Al_2O_3.

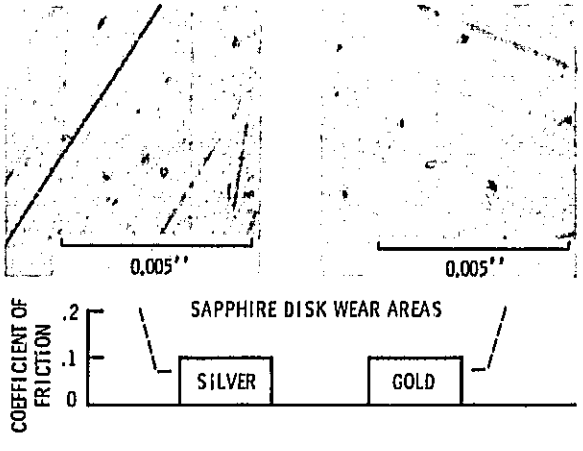

Figure 3. - Coefficient of friction for gold and silver riders sliding on sapphire in vacuum (10^{-10} torr). Sliding velocity, 0.013 cm/s; ambient temperature, 25°; furation, 1 hr.

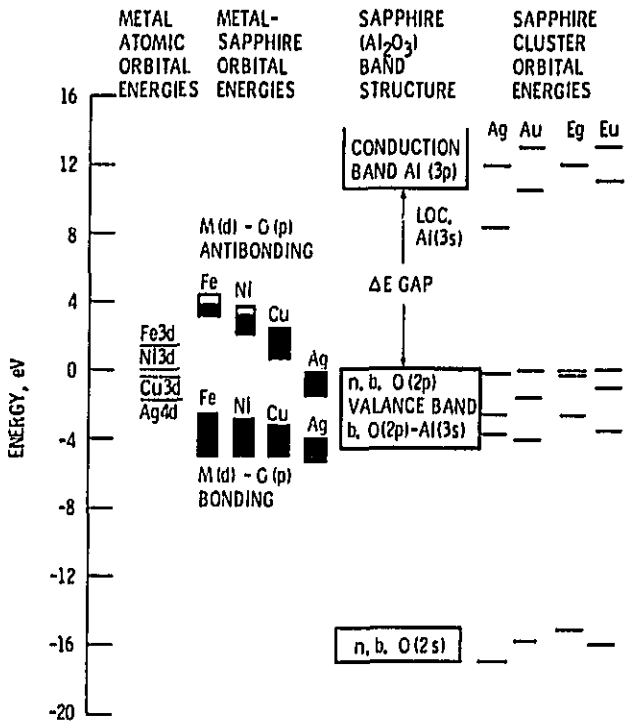

Figure 4. - Molecular-orbital energies, as determined by the self-consistent-field X-alpha scattered wave method, for clusters representing bulk sapphire and metal-sapphire interfaces.

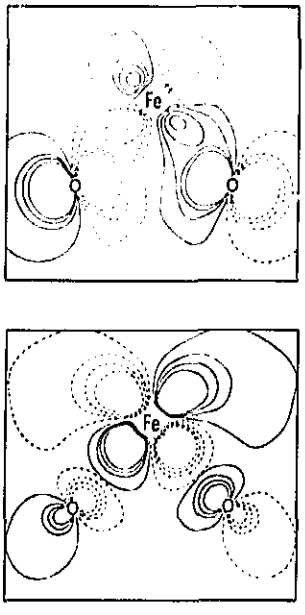

Figure 5. - Occupied bonding and unoccupied antibonding Fe(d)-O (p) molecular-orbital wave function contour maps for andiron atom supported on sapphire, plotted in the plane of the iron atom and two surface oxygen atoms. The solid and dashed contours represent the positive and negative phases of the wave function.

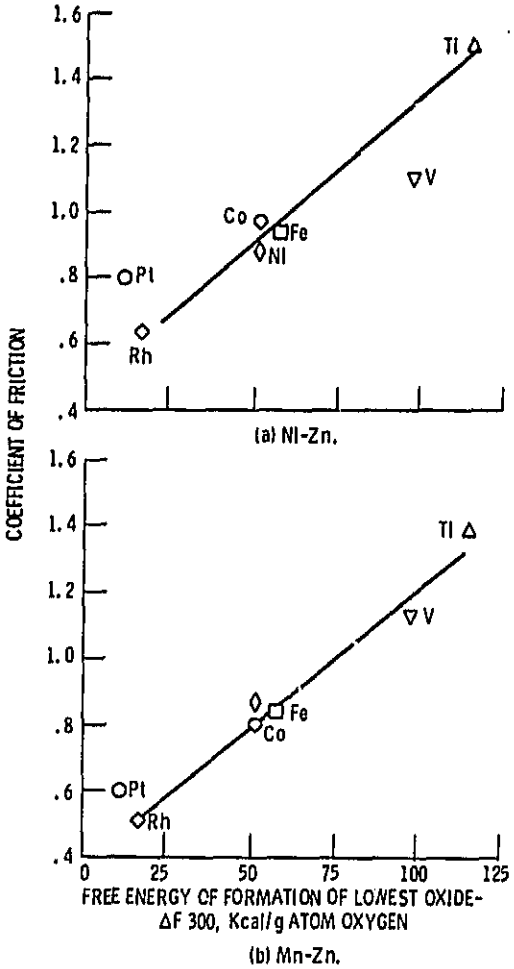

Figure 6. - Coefficients of friction for various metals in contact with ferrites as a function of the free energy of formation of the lowest oxide. Single-pass sliding; sliding velocity, 3 mm/min load, 0.05 to 0.2 N; vacuum, 30 nPa; room temperature.

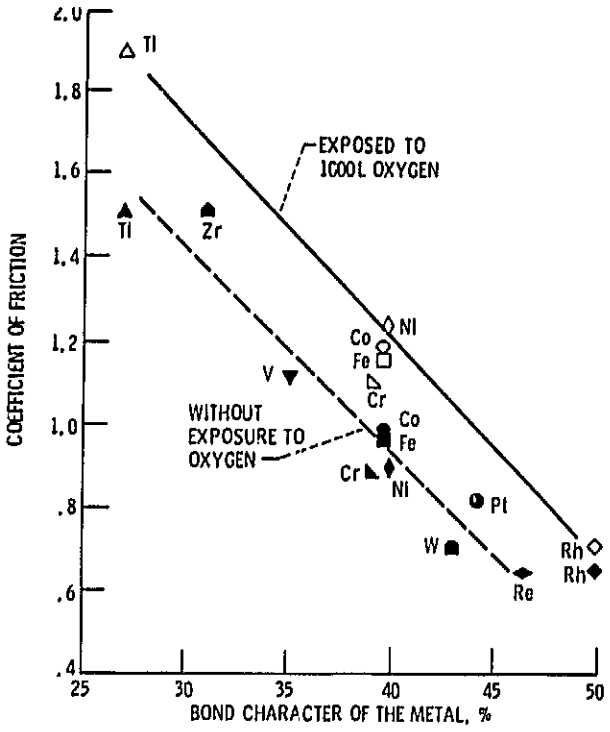

Figure 7. - Effect of adsorbed oxygen on the friction for various metals in contact with Ni-Zn ferrite. Exposure, 1000 L of oxygen gas; sliding velocity, 3 mm/min; load, 0.05 to 0.2 N; vacuum, 30 nPa; room temperature.

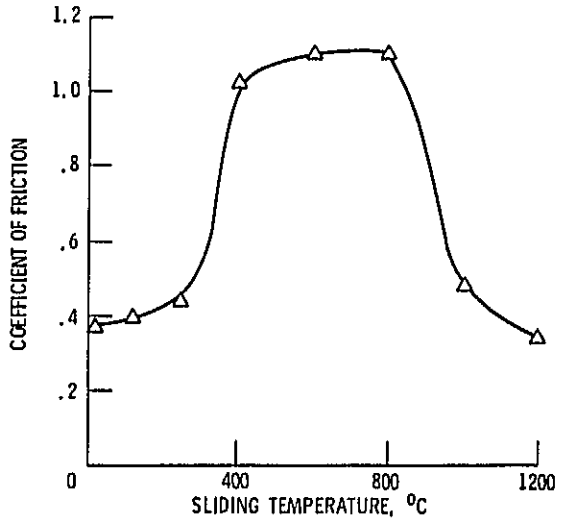

Figure 8. - Effect of temperature on coefficient of friction for sintered polycrystalline silicon carbide surface sliding against clean iron rider (which was argon-ion-sputter cleaned before experiments). Normal load, 0.1 to 0.2 N; vacuum, 30 nPa.

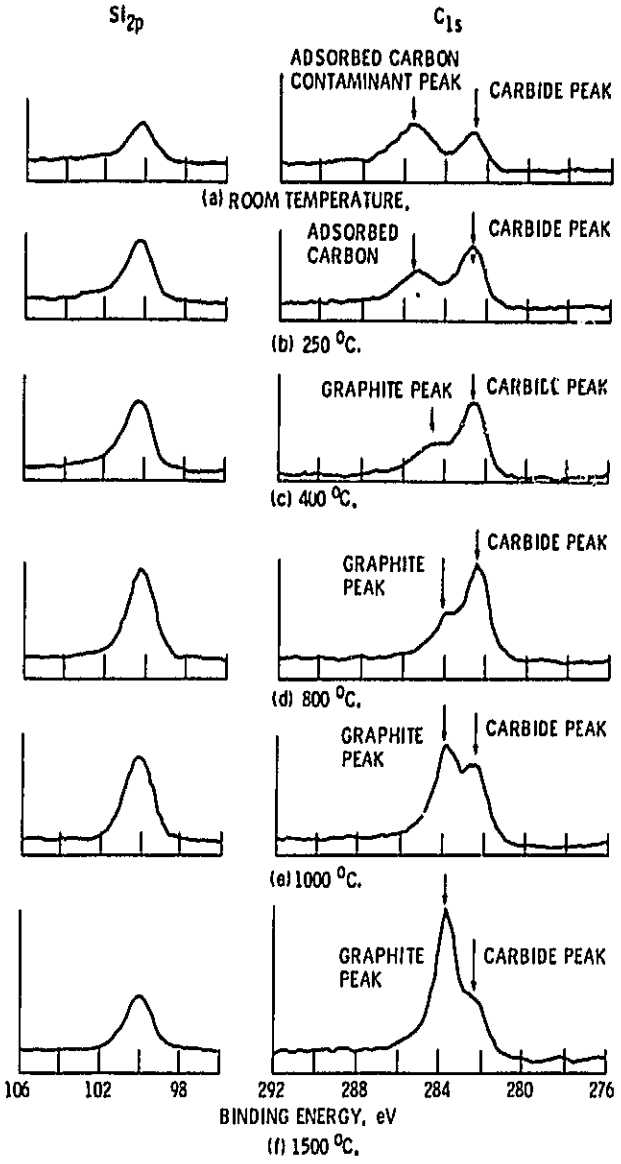

Figure 9. - Representative Si_{2p} and C_{1s} XPS peaks on silicon carbide (0001) surface preheated at various temperatures to 1500 °C.

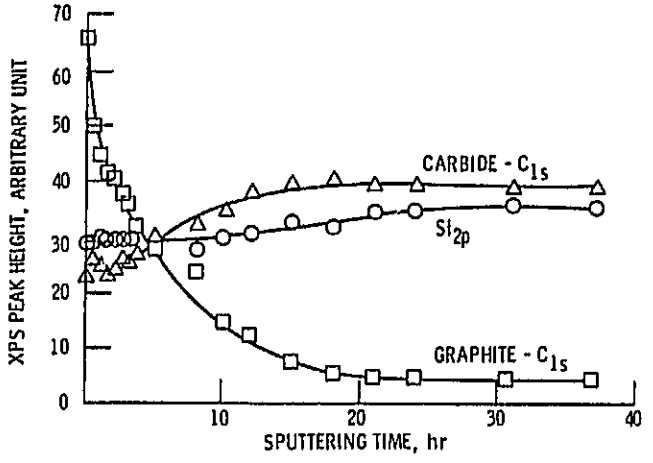

Figure 10. - Elemental depth profile of silicon carbide (0001) surface preheated at temperature 1500 °C for 1 hour.

(a) Hexagonal cracking.

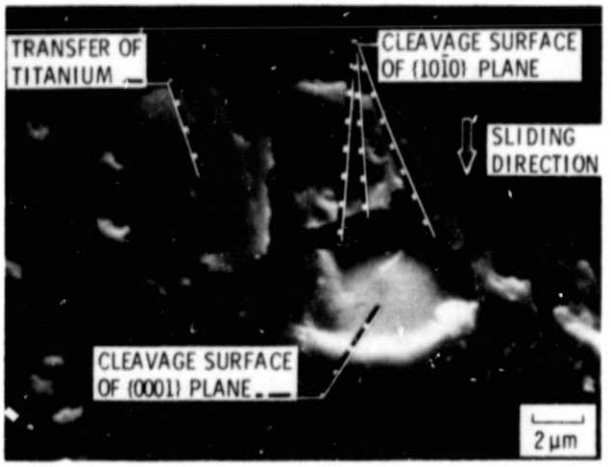

(b) Hexagonal pit.

Figure 11. - Scanning electron photomicrographs of wear tracks on the (0001) surface of single-crystal SiC in contact with rhodium and titanium as a result of ten passes of a rider in vacuum. Sliding direction, (10$\bar{1}$0); sliding velocity, 3 mm/min; load, 0.3 N; room temperature; pressure, 10^{-8} Pa; metal pin rider, 0.79 mm radius.

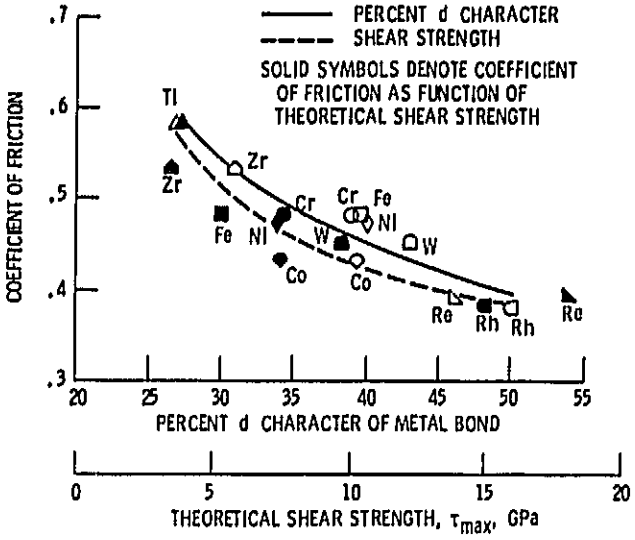

Figure 12. - Coefficients of friction as function of percent of metal d bond character and theoretical shear strength of metals in contact with silicon carbide (0001) surface in vacuum. Sliding direction, $<10\bar{1}0>$; sliding velocity, 3×10^{-3} m/min; load, 0.05 to 0.5 N; room temperature; vacuum pressure, 10^{-8} Pa.

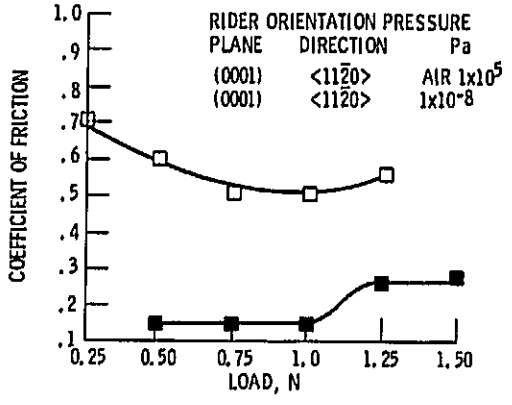

Figure 13. - Coefficient of friction as function of load for sapphire sliding on sapphire in vacuum, 30 nPa and air, 1×10^{5} Pa. Sliding velocity, 0.13 centimeter per second; temperature, 298 K; specimen outgassing with electron gun at 573 K. Disk specimen was (0001) plane parallel to sliding interface.

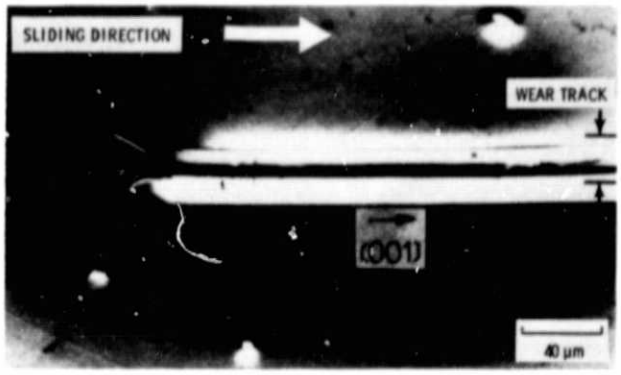

(a) In lubricant.

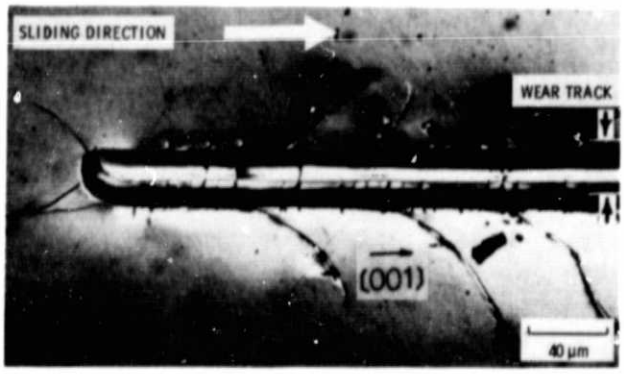

(b) In air.

Figure 14. - Scanning electron photomicrographs of wear tracks on single-crystal Mn-Zn ferrite (100) surface in sliding contact with 0.1 - mm - radius hemispherical diamond rider in lubricant (olive oil) and in air.